A Novel Network Architecture for C/U-Plane Staggered Handover in 5G Decoupled Heterogeneous Railway Wireless Systems

Li Yan, *Student Member, IEEE*, Xuming Fang, *Senior Member, IEEE*, and Yuguang Fang, *Fellow, IEEE*

***Abstract*— Previously, we proposed a broadband fifth-generation (5G) control/user (C/U)-plane decoupled heterogeneous railway wireless system to meet the exponentially increasing capacity demands in railway. Nevertheless, service interruptions due to the handovers in overlapping registration areas are still challenging in railway wireless systems. How to achieve soft and fast handovers to overcome these challenges attracts intensive attention finally. In this paper, we propose a novel network architecture for 5G C/U-plane decoupled heterogeneous railway wireless systems to physically separate and stagger the C-plane and U-plane handovers. During the C-plane handover process that occurs between the macro-cells, the U-plane is always kept connected without any handover, which achieves non-interruptible soft handover. Moreover, since there are no handovers in the U-plane, the handover procedure is significantly simplified, thereby accelerating the handover process. Similarly, during the U-plane handover process, which happens between the small cells, the C-plane is kept connected all the time, saving the otherwise intensive C-plane handover signaling. Besides, the coordinated multi-point transmission and reception (CoMP) and bi-casting technologies are applied to establish the target U-plane connection ahead of cutting off the old one, so that no interruption occurs during the U-plane handover process. This paper demonstrates that the proposed handover schemes can greatly improve the handover performance.**

***Index Terms*— 5G, C/U-plane, network architecture, handover, railway wireless systems.**

I. Introduction

RECENTLY, owing to the stronger transportation capability, lower energy consumption, less environment pollution and higher safety, the railway industry is ushering in a period of rapid development. With the vigorous growth of train transportation volume, exponentially increasing wireless services generated by passengers will occupy a high share in mobile communication markets in the future, which has catalyzed the study of next generation railway wireless systems to meet the wireless capacity demands on trains [1]–[3]. Because of explicit limitations on interference level and coverage which enable dependable service quality and efficient mobility support, lower frequency bands are usually the first choice for operators. Nevertheless, with the rapid development of wireless communications, these spectra have already been fully utilized. In public mobile networks, to meet the exponentially increasing capacity demands, the fifth-generation (5G) cellular systems would exploit higher frequency bands, including frequency bands higher than 5GHz, up to 300GHz, to gain broader spectra [4]–[6]. Unfortunately, the severer propagation loss of these bands heavily limits the signal coverage, which causes more frequent handovers or access failures. The subsequently generated signaling traffic is a huge burden for networks and user equipments (UEs) [7]. To increase the system capacity while mitigating network access signaling, the control/user (C/U)-plane decoupled architecture (details will be presented in Section II) may be a potential solution [8].

In our previous work [9]–[12], based on the evolution tendency of wireless communications for high-speed railway, we have started the research on C/U-plane decoupled heterogeneous railway wireless systems aiming at improving the train-ground wireless communication performance for future high-speed railway, such as Chinese high-speed railway. In [9] and [10], we investigate the design considerations of C/U-plane decoupled heterogeneous railway wireless systems and redesign the channel mappings and physical layer frames for this system. In [11], we propose a novel collaborative hybrid automatic repeat request (HARQ) scheme to reduce the retransmission latency of this system. And in [12], we present a dual-scheduler scheme to improve the resource utilization for this system. In this paper, to realize soft and fast handover, we propose a novel network architecture for C/U-plane decoupled heterogeneous railway wireless systems to physically separate and stagger the C-plane and U-plane handovers. In such networks, to address the large penetration loss and group handover signaling storm, a wireless access point (AP) and an onboard mobile relay (MR) are configured on the roofs inside and outside the train, respectively [5], [13]. Train passengers' equipments inside the train firstly access the AP and then their services are forwarded to wayside eNodeBs (eNBs) via the MR. According to [13], the links between the MR and wayside eNBs are the primary capacity bottleneck. Hence, the C/U-plane decoupled architecture is applied to these links

Manuscript received October 21, 2016; revised March 16, 2017; accepted March 17, 2017. Date of publication April 12, 2017; date of current version December 7, 2017. The work of L. Yan and X. Fang was supported in part by NSFC under Grant 61471303, in part by NSFC-Guangdong Joint Foundation under Grant U1501255, in part by the 973 Program under Grant 2012CB316100, in part by the Program for Development of Science and Technology of China Railway Corporation under Grant 2013X016-A, and in part by the EP7-PEOPLE-2013-IRSES Project under Grant 612652. The work of Y. Fang was supported by the U.S. National Science Foundation under Grant CNS-1343356. The Associate Editor for this paper was H. Dia.

L. Yan and X. Fang are with Key Laboratory of Information Coding and Transmission, Southwest Jiaotong University, Chengdu 610031, China (e-mail: liyan12047001@my.swjtu.edu.cn; xmfang@swjtu.edu.cn).

Y. Fang is with the Department of Electrical and Computer Engineering, University of Florida, Gainesville, FL 32611 USA (e-mail: fang@ece.ufl.edu).

Color versions of one or more of the figures in this paper are available online at http://ieeexplore.ieee.org.

Digital Object Identifier 10.1109/TITS.2017.2685426

and then the whole train can be regarded as a single user. In 5G C/U-plane decoupled heterogeneous railway wireless systems, to increase the capacity, the C-plane and U-plane of services are decoupled and distributed to different frequency bands. To enable reliable transmission and efficient mobility support, the relatively critical C-plane is kept at existing high-quality lower frequency bands in macro cells. To gain broader spectra, the corresponding U-plane, which is the data carrier thereby demanding more capacity, is moved to small cells operating at higher frequency bands. According to [14], macro cells usually have a coverage distance of about several kilometers, while small cells range around hundreds of meters. It should be noted that to facilitate the understanding we take the popular long term evolution (LTE) network as a baseline to analyze the proposed schemes of this paper.

Generally speaking, there are two types of handovers, i.e., the hard handover and the soft handover. In the hard handover, before a UE establishes a new U-plane connection with a target eNB (T-eNB), the old U-plane connection with the source eNB (S-eNB) is disconnected, which causes a transient interruption. While for the soft handover, the U-plane connection with the T-eNB is established before disconnecting with the old one. Currently, due to the implementation simplicity, only hard handover is supported in LTE networks [15]. Under high-speed mobility environments, more frequent handovers will be triggered. The consequently increasing interruptions will severely impact the quality of service (QoS). Moreover, in railway scenarios, a high-speed train passes through the overlapping area so fast that the handover procedure perhaps cannot be completed timely, resulting in frequent handover failures [16]. Hence, for railway wireless systems, soft and fast handover schemes are urgently needed to deal with such challenges.

In 5G C/U-plane decoupled heterogeneous railway wireless systems, the C-plane and U-plane are inherently separated into different physical nodes for transmissions. Based on this observation, to develop efficient soft and fast handover mechanisms, we propose a novel network architecture to physically separate and stagger the C-plane and U-plane handovers. Under this network architecture, the C-plane handover takes place between two adjacent macro cells, which is also called the inter-macro-cell handover. The U-plane handover is triggered in the overlapping area of two adjacent small cells, which is also called the inter-small-cell handover. Based on [17], the general overlapping area distance of macro cells in railway scenarios is also about hundreds of meters with a comparative size as that of the coverage of small cells. Therefore, it is reasonable to elaborately deploy a small cell in overlapping areas of macro cells. In this way, the inter-macro-cell and inter-small-cell overlapping areas are staggered which makes it possible to physically separate and stagger the C-plane and U-plane handovers. During the whole inter-macro-cell (C-plane) handover process, because of the elaborately deployed small cell in the inter-macro-cell overlapping area, the U-plane can be always kept connected without any handover. Subsequently, no communication interruption occurs at all. Moreover, without the need to hand over the U-plane, the handover procedure is simplified and less time is required to complete the handover procedure, which achieves fast handover in the C-plane.

Similarly, thanks to the elaborately staggered inter-macro-cell and inter-small-cell overlapping areas under this novel network architecture, during the inter-small-cell handover process, the C-plane is kept connected all the time without any handover. The otherwise intensive C-plane handover signaling is saved and the fast handover is achieved. With the C-plane kept connected, the inter-small-cell handover is equivalent to the conventional simple intra-eNB handover. To realize soft handover in the U-plane, a coordinated multi-point transmission and reception (CoMP) and Bi-casting based inter-small-cell handover scheme is designed. Before the handover, the serving gateway (SGW) dually casts the same U-plane data to these two adjacent small cells, which is called Bi-casting. Then, through CoMP, the two small cells simultaneously transmit these U-plane data to the MR. In this way, the new U-plane connection with the target small cell (T-small-cell) is established in advance and the communication interruption is avoided in the following handover process. Generally, during the joint transmission of CoMP, the coordinating eNB just transmits the U-plane data at the same time-frequency resource as that of the serving eNB, and the UE only receives the C-plane signaling from the serving eNB [18]. However, in conventional networks, the C-plane signaling and U-plane data are mixed up in the physical layer frame, intensive X2 signaling between the coordinating and serving eNBs is required so that these two eNBs can exactly align their transmission resources. Obviously, the conventional C/U-plane coupled architecture severely affects the flexibility of CoMP. This issue is fortunately avoided in the 5G C/U-plane decoupled heterogeneous railway wireless system. Since the U-plane is completely separated from the C-plane and moved to another frequency bands, it is much easier for the coordinating and serving eNBs to precisely align their U-plane transmission resources.

Based on the above descriptions, we can find that there will be more than one base stations simultaneously serving a MR in the 5G C/U-plane decoupled heterogenous railway wireless system. According to [19], the cross-correlated shadow fading model can be employed for theoretical analyses in such networks. In this paper, we use three performance metrics to evaluate the performance of the proposed C/U-plane staggered handover schemes, which are described below:

- **Communication outage probability**: defined as the joint outage probability of the C-plane and U-plane, which depends on both the received C-plane and U-plane signal quality. If either of them is lower than the outage threshold, the communication outage will happen. In this paper, this metric is used to depict the data transmission performance during handovers.
- **U-plane channel capacity**: defined as the U-plane data carrying capability. As the signaling on the C-plane is used to control the U-plane data transmission but contains no substantial content, for simplicity the C-plane signaling carrying capability is not considered in this paper. Nevertheless, it should be noted that C-plane capacity is also an important factor that limits the network performance. In [10], we have studied the bandwidth

matching problem between the C-plane and the U-plane. The analysis results show that with lower frequency bands totally allocated to the C-plane, a high C-plane capacity can be achieved.

- **Handover success probability**: defined as the probability that the actual handover, no matter whether it is in C-plane or in U-plane, is successful. For instance, in the conventional LTE-based handover scheme, the U-plane is totally interrupted during the whole handover execution phase. After the C-plane is handed over to the T-eNB, the U-plane is rebuilt. From the perspective of the air interface signaling, the conventional LTE-based handover is equivalent to the C-plane handover. Hence, the handover success probability of the conventional LTE-based handover scheme depends on the C-plane signal quality. Based on this observation, we can find that handover success probability and communication outage probability are two quite different metrics. As aforementioned, communication outage probability can better reflect the data transmission performance. Unlike handover success probability, communication outage probability depends on both the C-plane and the U-plane signal qualities. Only when both the C-plane control signaling data and the U-plane user data are all correctly received, can the communication be identified as connected.

In the proposed inter-small-cell handover scheme (U-plane handover, the expressions of "inter-small-cell handover" and "U-plane handover" are used interchangeably in this paper), the CoMP and Bi-casting technologies enable the MR to simultaneously keep two U-plane connections. The consequently enhanced U-plane signal quality improves the U-plane channel capacity and the handover success probability. Besides, under the novel network architecture where the inter-macro-cell and inter-small-cell overlapping areas are elaborately staggered, the inter-small-cell overlapping area corresponds to the interior areas of macro cells. The received C-plane signal is also of high quality, which greatly reduces the communication outage probability.

In this elaborately designed network architecture, to physically separate and stagger the C-plane and U-plane handovers, a small cell that manages the U-plane is deployed in the overlapping area of two adjacent macro cells. Hence, in the proposed inter-macro-cell handover scheme (C-plane handover, the expressions of "inter-macro-cell handover" and "C-plane handover" are used interchangeably in this paper), the received U-plane signal is of high quality, thereby reducing the communication outage probability and enhancing the U-plane channel capacity. From the perspective of the signal quality, the proposed inter-macro-cell handover scheme attains the same handover success probability as that of the conventional LTE-based handover scheme.

The rest of this paper is organized as follows. Section II overviews the conventional LTE-based handover scheme. Section III describes the proposed C/U-plane staggered handover schemes in detail. Section IV presents the used channel models. Section V gives the theoretical performance evaluation of different handover schemes. Section VI illustrates the numerical simulation results. Finally, Section VII concludes the paper.

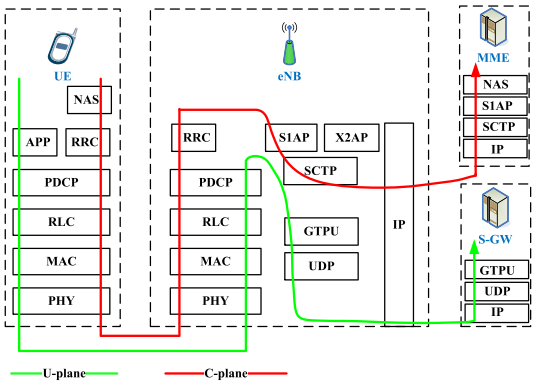

Fig. 1. Upper layer decoupled C-plane and U-plane flows in conventional LTE networks.

II. Conventional LTE-Based Handover Scheme

A. Upper Layer Decoupled LTE Networks

In LTE networks, there are two planes established between the accessing UE and the serving eNB, i.e., the C-plane and U-plane. As shown in Fig. 1, one of the most important design principles in LTE networks is to split design space into C-plane and U-plane in upper layers [20]. Through totally different upper stack protocols, the user dedicated data are transmitted on the U-plane from or to the SGW, while the control signaling designed for network access is transmitted on the C-plane from or to the mobility management entity (MME). Nevertheless, as shown in Fig. 1, in conventional LTE networks, the upper layer decoupled C-plane and U-plane still share the same lower stack protocols. That is, they still share the same physical network node for transmissions. To increase the system capacity while guaranteeing the mobility performance and transmission reliability, the further physically decoupling architecture is needed. Hence, in the C/U-plane decoupled architecture, according to the diverse requirements of the C-plane and U-plane, they are decoupled and distributed to different network nodes operating at different frequency bands that can meet their requirements.

B. Hard Handover Scheme in Conventional LTE Networks

In conventional LTE networks, only the hard handover scheme is supported. once a handover is triggered, the U-plane connection with an S-eNB will be cut off. After the new C-plane connection with the T-eNB is established, a new U-plane connection with the T-eNB will be rebuilt. Obviously, because of the upper-layer decoupled C-plane and U-plane design principle, the C-plane and U-plane handovers are functionally separated in conventional LTE networks. Nevertheless, as the C-plane and U-plane are still physically coupled in this network, the C-plane and U-plane handovers concurrently take place in the same physical node. The detailed LTE-based handover procedure is depicted in Fig. 2 [21]. Generally, the hard handover process consists of three operational phases, i.e., the handover preparation phase, the handover execution phase and the handover completion phase.

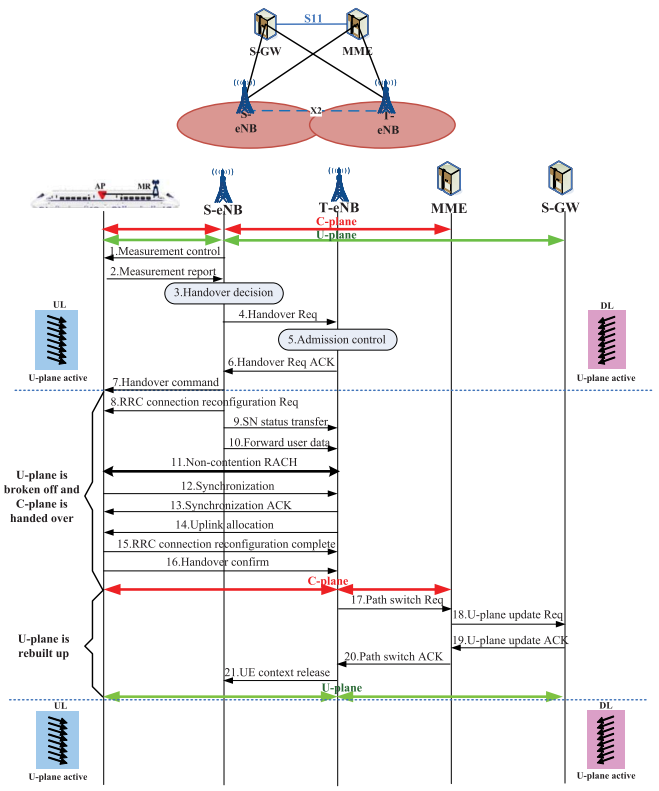

Fig. 2. Signaling procedure of the conventional LTE-based handover scheme.

In Fig. 2, the steps 1∼6 take place in the handover preparation phase. Based on the measurement reports from a UE, the S-eNB decides whether or not to hand over the UE to the T-eNB. It is notable that in linearly deployed railway wireless systems, based on the moving direction of a train, the T-eNB is supposed to know in advance. If the handover is successfully triggered, a handover request message will be sent to the T-eNB to pass necessary information for the handover resource preparation in the T-eNB. If the available resources in the T-eNB cannot afford all bearers of the UE, some bearers will be rejected during the admission control process. Finally, the admission results carried by the acknowledgement message are sent to the S-eNB.

When the UE receives the handover command message from the S-eNB, the handover procedure gets into the handover execution phase, in which the U-plane is totally interrupted and almost all air interface signaling is used to establish the new C-plane connection with the T-eNB. Through the non-contention random access procedure (it should be noted that the non-contention based part of random access is usually used in handover [22]), the UE attempts to access and synchronize to the T-eNB. If it succeeds, a handover confirmation message will be sent to the T-eNB, which implies that the new C-plane connection with the T-eNB is established. As a part of the handover execution phase, the remaining downlink U-plane data of the S-eNB are forwarded to the T-eNB. Usually, the forwarding process can be concurrently finished during the handover signaling procedure. Hence, the time consumption of forwarding is not included in the total time consumption of the handover execution phase. According to [22], the minimum total time consumption, including the time consumption of synchronization and signaling processing, is 25ms.

The U-plane rebuilding is performed in the following handover completion phase which corresponds to the steps 17∼21. Since the UE moves to a new cell, its U-plane path needs to be updated. After the path switch process, the UE context in the S-eNB is released and the new U-plane connection with the T-eNB is established. According to [22], the minimum time consumption of this phase is about 35ms. Based on the above analysis, we observe that during the whole hard handover process of conventional LTE networks, the U-plane is interrupted for at least 60ms, which severely impacts the quality of experience (QoE) of a user. Even worse, under high-speed mobility environments, frequent handovers result in frequent interruption and further degrade the service quality. Suppose the moving speed of a train is 360km/h, and the coverage radius of the eNB is 2km. The time spent by the train passing through a cell is approximately 40s. If the average call holding time is 2min, then four handovers will be triggered, that is, four interruptions will occur during this call. Such frequent interruptions seriously degrade the QoE of a user.

As alluded earlier, in LTE networks, the C-plane and U-plane are upper layer decoupled. From the above analysis of the LTE-based handover procedure, we observe that the U-plane and C-plane handovers are functionally separated. In the handover execution phase, the U-plane is cut off and almost all the signaling is used for the C-plane handover. After the new C-plane is established, the U-plane will be rebuilt in the following handover completion phase. Hence, from the perspective of the air interface signaling, the whole handover execution phase is equivalent to the C-plane handover. Based on this observation, to realize soft and fast handovers, a novel network architecture is proposed to physically separate and stagger the C-plane and U-plane handovers for the 5G C/U-plane decoupled heterogeneous railway wireless systems in the following section.

III. C/U-Plane Staggered Handover Schemes

A. 5G C/U-Plane Decoupled Heterogeneous Railway Wireless Systems

In our previous works, we proposed a C/U-plane decoupled heterogeneous railway wireless network architecture to meet the tremendously increasing capacity demands in railway [9]–[12]. The detailed network architecture is depicted in Fig. 3. To provide a dependable connection for train passengers, a wireless AP and an onboard MR are configured on the roofs inside and outside the train, respectively. Firstly, train passengers' equipments connect to the AP and then their services are forwarded to wayside eNBs via the MR. In this paper, we focus on the links between the MR and wayside eNBs and the whole train is regarded as a single user, i.e., the MR. To gain broader spectra, the U-plane of passengers' services (converged in the MR), which demands more capacity, is moved to small cells operating at higher frequency bands. To enable efficient mobility support, the relatively more important C-plane is kept in macro cells operating at high-quality lower frequency bands. More precisely, some low-rate

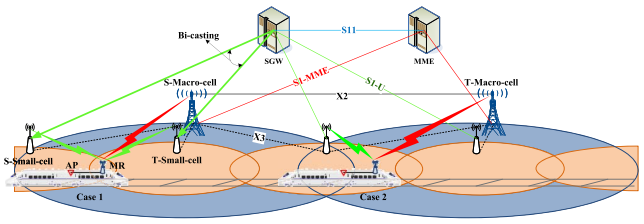

Fig. 3. The 5G C/U-plane decoupled heterogeneous railway wireless system. Case 1 is the Bi-casing and CoMP based inter-small-cell handover scenario and Case 2 is the inter-macro-cell handover scenario.

services with strict requirements for transmission reliability, e.g., the train control information, can be entirely distributed to macro cells without decoupling. In the future train control systems, more real-time monitoring equipments to ensure the train operational safety will be employed, which will generate more data to transmit between the train and wayside eNBs. To fulfill these capacity demands, less critical data can also be transmitted with the U-plane moved to higher frequency bands just as the passengers' services. Since small cells are only responsible for the U-plane, they are just connected to the SGW while not to the MME as shown in Fig. 3. The control signaling for managing small cells is handled by macro cells via interface X3. In order to provide some low-rate services that have strict requirements for transmission reliability, in addition to the MME, macro cells can also be connected to the SGW.

B. The Proposed C/U-Plane Staggered Handover Schemes

In this section, based on the 5G C/U-plane decoupled heterogeneous railway wireless system, we propose a novel network architecture to physically separate and stagger the C-plane and U-plane handovers which has been shown in Fig. 3 with Case 1 and Case 2 respectively illustrating the Bi-casing and CoMP based inter-small-cell handover scenario and the inter-macro-cell handover scenario. As depicted in Fig. 3 (to facilitate the understanding, three small cells are deployed within a macro cell in Fig. 3. For theoretical analyses in Section V, the number of small cells within a macro cell will be expanded to a general case.), a small cell providing the U-plane is elaborately deployed in the overlapping area of two adjacent macro cells. Then, the cell edge of the C-plane is no longer the cell edge of the U-plane. During the inter-macro-cell (C-plane) handover process, the U-plane can always be kept connected without any handover. Consequently, there is no U-plane interruption in the proposed inter-macro-cell handover. On the other hand, under this novel network architecture, the overlapping areas of any two adjacent small cells correspond to the interior areas of macro cells. Hence, during the inter-small-cell (U-plane) handover process, the C-plane can be kept connected all the time without any handover. With the connected C-plane, the U-plane handover is equivalently simplified to the conventional intra-eNB handover. As a result, based on the above design, the C-plane and U-plane handovers are completely separated. To avoid the U-plane interruption, a CoMP and Bi-casting based soft inter-small-cell handover scheme is used. Before entering a inter-small-cell overlapping

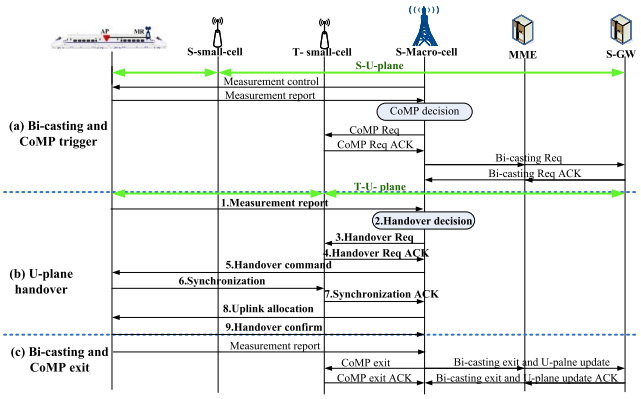

Fig. 4. Signaling procedure designed for the CoMP and B-casting based inter-small-cell (U-plane) handover scheme.

area, if the MR measures the received U-plane signal quality from the source small cell (S-small-cell) is lower than the preset threshold Γ_{CoMP}, CoMP and Bi-casting will be triggered. The two adjacent small cells begin to simultaneously transmit the same U-plane data to the MR. When the MR gets into the overlapping area, it can receive two U-plane signals from both of the S-small-cell and T-small-cell. With the early established U-plane connection to the T-small-cell, no U-plane interruption occurs during the inter-small-cell handover.

Accordingly, the signaling procedure of the proposed inter-small-cell handover scheme is designed as shown in Fig. 4. As discussed above, during the inter-small-cell handover, the C-plane is always kept connected without any handover. The whole CoMP and Bi-casting based U-plane handover process is divided into three operational phases, i.e., the CoMP and Bi-casting triggering phase, the U-plane handover phase and the CoMP and Bi-casting exit phase.

Considering the limited overlapping area problem under high-speed railway scenarios, by giving Γ_{CoMP} a value larger than that of the signal quality in the overlapping area, CoMP and Bi-casting will be triggered early before the train enters the overlapping area. It should be noted that in the C/U-plane decoupled architecture, only macro cells have the control ability. All control signaling is transmitted or forwarded via macro cells. In the CoMP and Bi-casting triggering phase, if the MR reports that the received U-plane signal quality from the S-small-cell is lower than Γ_{CoMP}, the macro cell (as the C-plane and U-plane handover scenarios are both depicted in Fig. 3, here the macro cell corresponds to the S-macro-cell in Fig.3) will inform the T-small-cell to activate CoMP. Upon receiving the CoMP Req ACK message from the T-small-cell, the macro cell asks the SGW to bi-cast the U-plane data both to the S-small-cell and T-small-cell. Then, an additional U-plane connection with the T-small-cell is established.

As the train enters the overlapping area and the received U-plane signal quality from the S-small-cell continuously decreases, the U-plane handover phase is activated. With the early established U-plane connection to the T-small-cell, no interruption occurs in the proposed inter-small-cell handover scheme, thus achieving the soft handover. Since in this scheme the C-plane is always connected without any handover, the otherwise intensive C-plane signaling, such as the

RRC rebuilding and non-contention random access signaling, is saved. Compared with the conventional LTE-based handover procedure in Fig. 2, the handover procedure of the proposed scheme in Fig. 4 is greatly simplified, facilitating the handover process.

As the train gets out of the overlapping area and runs towards the T-small-cell, the received signal quality from the T-small-cell gets increasingly better. If it is higher than Γ_{CoMP}, CoMP and Bi-casting are terminated. Similar with the first phase, the CoMP and Bi-casting exit phase doesn't occur in the overlapping area but after running out of it. Generally, the signal quality is measured through the reference signals (RSs). Although in the overlapping area the S-small-cell and T-small-cell use the same time-frequency resources to simultaneously transmit U-plane data for the MR, with orthogonal RSs employed in the two cells, their signal quality can still be separately measured. However, this is out of the scope of this paper.

Under this novel network architecture, a small cell providing the U-plane is elaborately deployed in the overlapping area of two adjacent macro cells. As a result, in the proposed inter-macro-cell (C-plane) handover scheme, the U-plane is kept connected all the time without any handover, thus achieving the soft handover. Accordingly, the inter-macro-cell handover signaling procedure is designed as shown in Fig. 5. If the measurement results meet the handover condition (e.g., the received signal quality from the T-macro-cell is hdB higher than that from the S-macro-cell), the C-plane handover will be triggered. With the connected U-plane, the admission control process in the conventional LTE-based handover scheme is saved, which also avoids the handover failure due to the lack of resources in the T-eNB. Similar to the conventional LTE-based handover procedure in Fig. 2, the MR needs to access and synchronize to the T-macro-cell through the non-contention random access process. Nevertheless, due to the connected U-plane, the downlink data forwarding and the U-plane path switch processes are saved. Hence, compared with Fig. 2, the handover procedure of the proposed inter-macro-cell handover scheme in Fig. 5 is greatly simplified, achieving fast handover.

Small-cell-based data offloading has been a non-controversial approach to enhance the capacity for future 5G wireless systems. Without the C/U-plane decoupled network architecture and the proposed handover schemes, the conventional LTE-based hard handover scheme may still be used for inter-small-cell and inter-macro-cell handovers, which will heavily degrade the system performance due to more frequent handovers and the subsequently aggravated signaling overhead especially for high-speed railway scenarios. Nevertheless, as described above, with the proposed handover schemes under the 5G C/U-plane decoupled heterogenous railway wireless system, the inter-small-cell and inter-macro-cell handover procedures are both greatly simplified, thereby mitigating the above problems.

For clarity, the time consumption of different handover schemes is summarized and compared as listed in TABLE I. To simplify the analysis, the time consumption of common signaling, e.g., the signaling of measurement control and measurement report, is not considered. Besides, HARQ retransmissions of signalling in [22] are also not considered. As aforementioned, the downlink data forwarding of the conventional LTE-based handover scheme can be concurrently completed during the handover signaling procedure. Hence, in TABLE I, the time consumption of items 4∼5 is not added in the total time consumption. In the inter-small-cell handover scheme, since the CoMP and Bi-casting triggering and exit phases do not take place in the overlapping area, and their time consumption cannot aggravate the limited overlapping area problem, thereby not included in the total time consumption calculation. Compared with the conventional LTE-based handover scheme, over 87.2% time is saved in the proposed inter-small-cell handover scheme, and over 56.4% time is saved in the proposed inter-macro-cell handover scheme. Obviously, the proposed schemes greatly accelerate the handover procedure, thereby mitigating the limited overlapping area problem in railway scenarios.

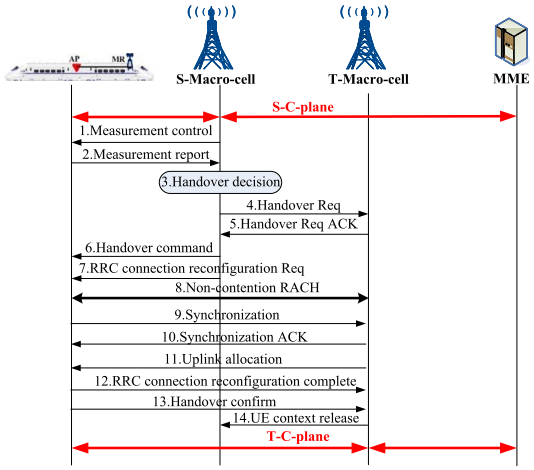

Fig. 5. Signaling procedure designed for the proposed inter-macro-cell (C-plane) handover scheme.

IV. Wireless Channel Models

A. SIR Model

Without loss of generality, let the signal propagation distance be x, the received signal power can be expressed as [23]

$$P_r(x)[dBm] = P_t - PL(x) - \varepsilon \tag{1}$$

where P_t denotes the eNB transmit power in dBm. ε is the shadow fading, generally modeled as a Gaussian random variable with mean zero and standard deviation σ, i.e., $\varepsilon \sim N\left(0, \sigma^2\right)$ [23]. $PL(x)$ represents the large-scale path loss in dB. Practically, for different frequency bands, $PL(x)$ is evaluated by different path loss models. In this paper, the large-scale path losses in higher and lower frequency bands are denoted by $PL_s(x)$ and $PL_m(x)$, respectively.

Based on the field test results in [24], co-channel interference has much more significant impact on the transmission reliability than noise for railway wireless systems. Consequently, for simplicity noise is neglected in following analyses. Suppose N_{eNB} eNBs reuse the same frequency band, the

TABLE I
TIME CONSUMPTION COMPARISONS /*ms*

No.	Signaling	Conventional LTE-based handover scheme	Proposed U-plane handover scheme	Proposed C-plane handover scheme
1	Admission control	T	0	0
2	Handover command	1	1	1
3	RRC connection reconfiguration Req	1	0	1
4	SN status transfer	T_{X2-C}	0	0
5	Forward user data	T_{X2-U}	0	0
6	Non-contention RACH	11	0	11
7	eNB processing delay	4	0	4
8	Synchronization	1	1	1
9	Synchronization ACK	1	1	1
10	Uplink allocation	1	1	1
11	UE processing delay	2.5	2.5	2.5
12	RRC connection reconfiguration complete	1	0	1
13	Handover confirm	1	1	1
14	Path switch Req	T_{S1-C} (2∼15ms)	0	0
15	MME processing delay	15	0	0
16	U-plane update Req	T_{S11}	0	0
17	SGW processing delay	10	0	0
18	U-plane update ACK	T_{S11}	0	0
19	Path switch ACK	T_{S1-C} (2∼15ms)	0	0
20	eNB processing delay	4	0	0
21	UE context release	1	0	1
	Time consumption	54.5+T+2T_{S1-C}+2T_{S11}	7.5	25.5

co-channel interference is given by

$$I[dBm] = 10\lg\left(\sum_{n=1}^{N_{eNB}} 10^{(P_t - PL_n)/10}\right) \tag{2}$$

where PL_n is the large-scale path loss experienced by the interference signal stemming from the nth co-channel eNB. Besides, to simplify the following theoretical analysis, shadowing fading is not considered in interference signals. Then, the received signal quality can be computed in the signal to interference ratio (SIR) form as

$$SIR(x)[dB] = P_r(x) - I \tag{3}$$

B. Cross-Correlated Shadow Fading Model

Shadow fading is a large-scale phenomenon which depends on surrounding communication environments. In the 5G C/U-plane decoupled heterogeneous railway wireless system, the macro cell (providing the C-plane) and small cell (providing the U-plane) deployed at different locations simultaneously serve the same train. According to [19], there are some common components between the propagation paths of macro and small cell signals, especially for the area near the train. As a consequence, the shadow fading of macro and small cells are cross-correlated. Based on [25], the cross-correlation of shadow fading can be explained by a partial overlap W_O of the large-scale propagation medium as shown in Fig. 6. The non-overlapping propagation areas W_N are considered independent. In the subsequent section, the cross-correlated shadow fading model will be frequently used. To avoid repetitive derivations, the unified results are given here. For different cases, it only needs to change the values of necessary parameters to get the corresponding model results.

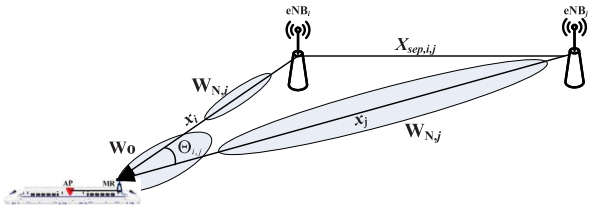

Fig. 6. Cross-correlated shadow fading.

According to [25] and [26], the shadow fading can be decomposed as

$$\varepsilon_i = W_O + W_{N,i} \tag{4}$$

where W_O and $W_{N,i}$ are independent Gaussian random variables with zero mean and standard deviations σ_{W_O} and $\sigma_{W_{N,i}}$, respectively. They satisfy

$$\begin{aligned} {\sigma_i}^2 &= {\sigma_{W_O}}^2 + {\sigma_{W_{N,i}}}^2 \\ E[\varepsilon_i \varepsilon_j] &= {\sigma_{W_O}}^2 = \rho_{i,j}\sigma_i\sigma_j \end{aligned} \tag{5}$$

According to [27], the cross-correlation coefficient of shadow fading can be modeled as

$$\rho_{i,j} = \rho_{j,i} = \begin{cases} \sqrt{\dfrac{\min(x_i, x_j)}{\max(x_i, x_j)}}, & 0 \le \Theta_{i,j} \le \Theta^T \\ \left(\dfrac{\Theta^T}{\Theta_{i,j}}\right)^{\gamma} \sqrt{\dfrac{\min(x_i, x_j)}{\max(x_i, x_j)}}, & \Theta^T < \Theta_{i,j} \le \pi \end{cases} \tag{6}$$

where γ is referred to as a parameter determined by the size and height of terrain and the height of base station, and is generally set to 0.3 [27]. Θ^T corresponds to the angle

threshold, defined as

$$\Theta^T = 2\arctan\left(\frac{d_{cor}}{2\min\left(x_i, x_j\right)}\right) \tag{7}$$

where d_{cor} is the serial de-correlation distance with value between 50m and 200m for suburban areas [28]. $\Theta_{i,j}$ in (6) is the angle between the propagation paths of two eNB signals as shown in Fig. 6, which can be derived as

$$\Theta_{i,j} = \arccos\left(\frac{{x_i}^2 + {x_j}^2 - {x_{sep,i,j}}^2}{2x_i x_j}\right) \tag{8}$$

Then, taking (8) into (6), we can obtain $\rho_{i,j}$. With $\rho_{i,j}$, the standard deviations σ_{W_O}, $\sigma_{W_{N,i}}$ and $\sigma_{W_{N,j}}$ in (5) can be worked out. From the above derivations, we can find that x_i, x_j and $x_{sep,i,j}$ are three necessary parameters to obtain the shadow fading decomposition results of any pair of base stations. Without loss of generality, we can get the correlation matrix for the case with K base stations serving a UE as

$$\Sigma = \begin{bmatrix} {\sigma_1}^2 & \sigma_1\sigma_2\rho_{1,2} & \cdots & \sigma_1\sigma_K\rho_{1,K} \\ \sigma_1\sigma_2\rho_{1,2} & {\sigma_2}^2 & \cdots & \sigma_2\sigma_K\rho_{2,K} \\ \vdots & \vdots & \ddots & \vdots \\ \sigma_1\sigma_K\rho_{1,K} & \sigma_2\sigma_K\rho_{2,K} & \cdots & {\sigma_K}^2 \end{bmatrix} \tag{9}$$

Then, the joint probability distribution function (PDF) of $\varepsilon_1, \varepsilon_2, \ldots, \varepsilon_K$ can be expressed as [29]

$$f_{\varepsilon_1,\varepsilon_2,\ldots,\varepsilon_K}(\varepsilon_1, \varepsilon_2, \ldots, \varepsilon_K) = \frac{1}{(2\pi)^{K/2} det(\sum)^{1/2}} e^{-\frac{1}{2}Z^T\Sigma^{-1}Z} \tag{10}$$

where $(\cdot)^T$ denotes the transportation, $det(\cdot)$ denotes the determinant and $Z^T = [\varepsilon_1, \varepsilon_2, \ldots, \varepsilon_K]$.

V. Performance Evaluation Models

Based on the above wireless channel models, performance evaluations for different handover schemes, including the communication outage probability, the U-plane channel capacity and the handover success probability in the overlapping areas, are analyzed in this section. Since the wireless networks under railway scenarios usually have a linear topology, especially for the most common viaduct scenarios [1], [30], as shown in Fig. 7 macro cells and small cells are deployed on straight lines with the vertical distances $d_{min,m}$ and $d_{min,s}$ to the rail, respectively. In Fig. 7, R_m, R_s, a_m and a_s,are the radiuses of macro cells, the radiuses of small cells, the inter-macro-cell overlapping area distance and the inter-small-cell overlapping area distance, respectively. The abscissa axes coinciding with the train driving direction are set to facilitate the computation in terms of train travel distance d. The origins of these axes correspond to the starting points of overlapping areas.

A. Performance Evaluation of the Conventional LTE-Based Handover Scheme

As shown in Fig. 7(a), to conduct the performance evaluation of the conventional LTE-based handover scheme, the whole overlapping area is divided into three components for the ease of analysis. Before the handover execution phase,

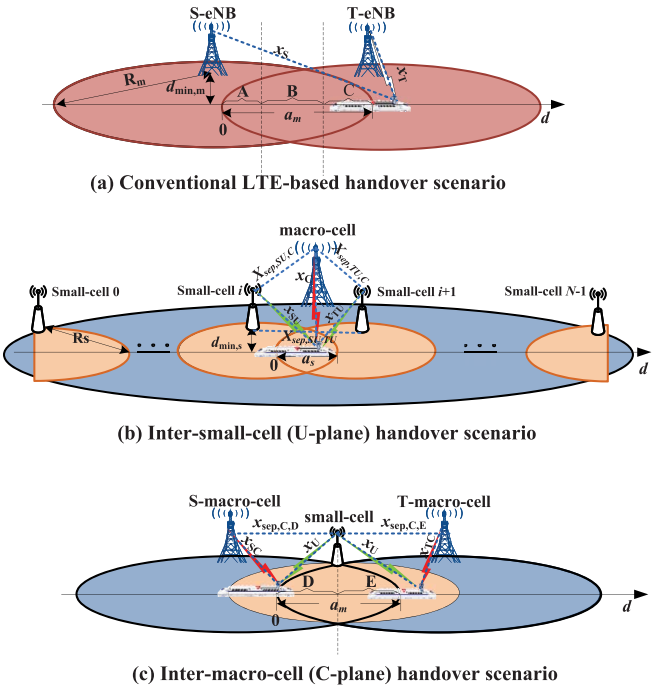

Fig. 7. Handover scenarios of different handover schemes.

in the area A, the MR still connects with the S-eNB. For simplicity, it is assumed that the handover takes place at the center of the overlapping area, i.e., the area B, in which the U-plane connection is totally interrupted. In the area C, the whole handover procedure is completed and the MR has built the connection with the T-eNB. Suppose the time consumption of the handover is T_h and the train's moving speed is v. Then, the distance of the area B is $T_h \times v$. The area A and C have the same distance, which can be expressed as $\frac{a - T_h \times v}{2}$.

Area A: In the area A, the MR receives signals from the S-eNB. Suppose the train starts from the origin and travels through distance d, then the signal propagation distance can be expressed

$$x_S(d) = \sqrt{(d + R_m - a_m)^2 + {d^2}_{\min,m}} \tag{11}$$

As aforementioned, the communication outage probability is defined as the complementary probability of the event that both the C-plane and U-plane signal quality is higher than the outage threshold, that is,

$$\begin{aligned} P_{out,A}(d) &= 1 - P(SIR(x_S(d)) > \Gamma)^2 \\ &= = 1 - P\left(P_{t,m} - PL_m(x_S(d)) - \varepsilon_S - I_S > \Gamma\right)^2 \\ &= 1 - \Phi^2\left(\frac{P_{t,m} - PL_m(x_S(d)) - \Gamma - I_S}{\sigma_S}\right) \end{aligned} \tag{12}$$

where Γ denotes the outage threshold. For simplicity, the outage thresholds of the C-plane and U-plane are set to the same value and $\Phi(x) = \frac{1}{\sqrt{2\pi}}\int_{-\infty}^{x} e^{-\frac{t^2}{2}}dt$.

Since the service data are carried by the U-plane, for study purpose in this paper we use Shannon capacity as the capacity of the U-plane. Let the U-plane bandwidth of the

conventional coupled network be $B_{coupled}$, then the U-plane channel capacity in the area A is given by

$$C_A(d) = B_{coupled}\log_2\left(1 + 10^{SIR(x_S(d))/10}\right) \tag{13}$$

Area B: As discussed before, in the hard handover execution phase, the U-plane is totally interrupted. Hence, the communication outage probability in the area B is 1, that is,

$$P_{out,B}(d) = 1 \tag{14}$$

Correspondingly, the U-plane channel capacity is

$$C_B(d) = 0 \tag{15}$$

Area C: After completing the handover, the MR has built the connection with the T-eNB. The signal propagation distance between the MR and T-eNB is

$$x_T(d) = \sqrt{(R_m - d)^2 + d^2_{\min,m}} \tag{16}$$

Then, the communication outage probability in the area C can be expressed as

$$\begin{aligned} P_{out,C}(d) &= 1 - P(SIR(x_T(d)) > \Gamma)^2 \\ &= 1 - \Phi^2\left(\frac{P_{t,m} - PL_m(x_T(d)) - \Gamma - I_T}{\sigma_T}\right) \end{aligned} \tag{17}$$

The U-plane channel capacity in the area C is given by

$$C_C(d) = B_{coupled}\log_2\left(1 + 10^{SIR(x_T(d))/10}\right) \tag{18}$$

During the conventional LTE-based handover process, almost all the air interface signaling is used for the C-plane reestablishment. More precisely, the C-plane is the real one on which the handover happens. Hence, from the perspective of the air interface signal quality, the handover success probability of the conventional LTE-based handover scheme is determined by the received C-plane signal quality. Generally, the handover success probability can be computed as the joint probability of two events that the handover is smoothly triggered and after the handover the wireless signals from the T-eNB can still be correctly received, which can be calculated as

$$P_{success}(d) = P_{HO}(d) \cdot P(SIR(x_T(d)) > \Gamma) \tag{19}$$

where $P_{HO}(d)$ represents the handover triggering probability. Under the handover triggering threshold h, $P_{HO}(d)$ can be given by

$$\begin{aligned} &P_{HO}(d) \\ &= P(\mathrm{P}_r(x_T(d)) - \mathrm{P}_r(x_S(d)) > h) \\ &= P(PL_m(x_S(d)) - PL_m(x_T(d)) + \varepsilon_S - \varepsilon_T > h) \\ &= \int_{-\infty}^{\infty} P(PL_m(x_S(d)) - PL_m(x_T(d)) + \varepsilon_0 - h > \varepsilon_T \\ &\quad |\varepsilon_S = \varepsilon_0) \times P(\varepsilon_S = \varepsilon_0)\, d\varepsilon_0 \\ &= \int_{-\infty}^{\infty} \Phi\left(\frac{PL_m(x_S(d)) - PL_m(x_T(d)) + \varepsilon_0 - h}{\sigma_T}\right) \\ &\quad \times \frac{e^{-\frac{\varepsilon_0^2}{2\sigma_S^2}}}{\sigma_S\sqrt{2\pi}} d\varepsilon_0 \end{aligned} \tag{20}$$

In (17), $P(SIR(x_T(d)) > \Gamma)$ indicates the probability that after the MR is handed over to the T-eNB, the wireless signals can still be correctly received. Based on (12) and (17), it is easy to get the expression of $P(SIR(x_T(d)) > \Gamma)$, which is not repetitively given here.

B. Performance Evaluation of the Proposed Inter-Small-Cell (U-Plane) Handover Scheme

The analysis scenario of the proposed CoMP and Bi-casting based soft inter-small-cell handover scheme is depicted in Fig. 7(b), in which N small cells are deployed within a macro cell. Without loss of generality, suppose that the MR are moving through the overlapping area between the $i\ th$ ($i = 0, 1, 2, \ldots N-1$) and $i{+}1\ th$ small cells. As shown in Fig. 7(b), the MR simultaneously keeps connections with three eNBs in the overlapping area. In addition to the macro cell which provides the C-plane for the MR, the two small cells concurrently offer the U-plane data for the MR, where the source U-plane (S-U-plane) signal and the target U-plane (T-U-plane) signal are provided by $i\ th$ small cell and the $i{+}1\ th$ small cell, respectively. According to Fig. 7(b), the values of the necessary parameters used in the aforementioned cross-correlated shadow fading model can be calculated as

$$\begin{aligned} x_{sep,SU,TU} &= 2R_s - a_s \\ x_{sep,SU,C} &= \sqrt{(d_{\min,m} - d_{\min,s})^2 + [(2R_s - a_s)\cdot(\frac{N-1}{2} - i)]^2} \\ x_{sep,TU,C} &= \sqrt{(d_{\min,m} - d_{\min,s})^2 + [(2R_s - a_s)\cdot(\frac{N-3}{2} - i)]^2} \\ x_C(d) &= \sqrt{[(2R_s - a_s)\cdot(\frac{N-3}{2} - i) + R_s - d]^2 + d^2_{\min,m}} \\ x_{SU}(d) &= \sqrt{(d + R_s - a_s)^2 + d^2_{\min,s}} \\ x_{TU}(d) &= \sqrt{(R_s - d)^2 + d^2_{\min,s}} \end{aligned} \tag{21}$$

Taking (21) into the above cross-correlated shadow fading model, we can get the correlation matrix for the scenario with three eNBs simultaneously serving the MR. In the inter-small-cell handover scheme, only when the C-plane signal quality and at least one of the two U-plane signal quality are higher than the outage threshold can the communication be kept connected. Hence, the communication outage probability of this scheme can be expressed as

$$\begin{aligned} &P_{out,U}(d) \\ &= P(SIR_C(x_C(d)) > \Gamma, SIR_{SU}(x_{SU}(d)) < \Gamma, \\ &\quad SIR_{TU}(x_{TU}(d)) < \Gamma) + P(SIR_C(x_C(d)) < \Gamma) \\ &= P(P_{t,m} - PL_m(x_C(d)) - I_C - \varepsilon_C > \Gamma, \\ &\quad P_{t,s} - PL_s(x_{SU}(d)) - I_{SU} - \varepsilon_{SU} < \Gamma, \\ &\quad P_{t,s} - PL_s(x_{TU}(d)) - I_{TU} - \varepsilon_{TU} < \Gamma) \\ &\quad + P(P_{t,m} - PL_m(x_C(d)) - I_C - \varepsilon_C < \Gamma) \\ &= \int_{-\infty}^{\zeta_C}\int_{\zeta_{SU}}^{\infty}\int_{\zeta_{TU}}^{\infty} f_{\varepsilon_C,\varepsilon_{SU},\varepsilon_{TU}}(\varepsilon_C, \varepsilon_{SU}, \varepsilon_{TU}) d\varepsilon_C d\varepsilon_{SU} d\varepsilon_{TU} \\ &\quad + Q\left(\frac{P_{t,m} - PL_m(x_C(d)) - I_C - \Gamma}{\sigma_m}\right) \end{aligned} \tag{22}$$

where $\zeta_C = P_{t,m} - PL_m(x_C(d)) - I_C - \Gamma$, $\zeta_{SU} = P_{t,s} - PL_s(x_{SU}(d)) - I_{SU} - \Gamma$, $\zeta_{TU} = P_{t,s} - PL_s(x_{TU}(d)) - I_{TU} - \Gamma$, and $Q(x) = \frac{1}{\sqrt{2\pi}} \int_x^\infty e^{-\frac{t^2}{2}} dt$.

In the proposed inter-small-cell handover scheme, CoMP and Bi-casting enable the MR to simultaneously receive two U-plane signals from both the S-small-cell and T-small-cell. Consequently,

$$SIR_{tot}(d)[W] = \frac{10^{\frac{SIR_{SU}(x_{SU}(d))+I_{SU}}{10}} + 10^{\frac{SIR_{TU}(x_{TU}(d))+I_{TU}}{10}}}{10^{\frac{I_{SU}}{10}} + 10^{\frac{I_{TU}}{10}}} \tag{23}$$

In C/U-plane decoupled heterogeneous railway wireless systems, higher frequency bands with broader spectra are exploited, that is, the supported bandwidth in this system denoted as $B_{decoupled}$, is much larger than that in conventional coupled wireless systems. Thus, the U-plane channel capacity in the overlapping area of the proposed inter-small-cell handover scheme can be expressed as

$$C_U(d) = B_{decoupled} \log_2(1 + SIR_{tot}(d)) \tag{24}$$

Because of the same reason that two U-plane signals can be received, the handover success probability in this scheme can be improved, which can be derived as

$$P_{success,U}(d) = P_{HO,U}(d) \cdot (1 - P(SIR_{SU}(x_{SU}(d)) < \Gamma, SIR_{TU}(x_{TU}(d)) < \Gamma)) \tag{25}$$

Based on similar argument as before, it is easy to get

$$\begin{aligned} &P_{HO,U}(d) \\ &= \int_{-\infty}^{\infty} \Phi\left(\frac{PL_s(x_{SU}(d)) - PL_s(x_{TU}(d)) + \varepsilon_0 - h}{\sigma_{W_{N,TU}}}\right) \\ &\quad \times \frac{e^{-\frac{\varepsilon_0^2}{2\sigma^2 W_{N,SU}}}}{\sigma_{W_{N,SU}}\sqrt{2\pi}} d\varepsilon_0 \end{aligned} \tag{26}$$

$$\begin{aligned} &P(SIR_{SU}(x_{SU}(d)) < \Gamma, SIR_{TU}(x_{TU}(d)) < \Gamma) \\ &= \int_{-\infty}^{\infty} \frac{e^{-\frac{t^2}{2\sigma^2 W_O}}}{\sigma_{W_O}\sqrt{2\pi}} Q\left(\frac{P_{t,s} - PL_s(x_{SU}(d)) - I_{SU} - t - \Gamma}{\sigma_{W_{N,SU}}}\right) \\ &\quad \times Q\left(\frac{P_{t,s} - PL_s(x_{TU}(d)) - I_{TU} - t - \Gamma}{\sigma_{W_{N,TU}}}\right) dt \end{aligned} \tag{27}$$

Taking (26) and (27) into (25), we can get the handover success probability of the proposed inter-small-cell handover scheme.

C. Performance Evaluation of the Proposed Inter-Macro-Cell (C-Plane) Handover Scheme

For simplicity, it is assumed that the C-plane handover happens at the center of the overlapping area. Subsequently, as shown in Fig. 7(c), the whole overlapping area is divided into two components for analysis. In the area D, the C-plane of the MR is provided by the S-macro-cell. While in the area E, it is provided by the T-macro-cell. As discussed before, thanks to the small cell which is elaborately deployed in the inter-macro-cell overlapping area, the U-plane is always kept connected without any handover during the whole inter-macro-cell handover process.

Area D: In the area D, the S-macro-cell and small cell serve the MR with the C-plane and U-plane connections, respectively. The values of the three necessary parameters in the cross-correlated shadow fading model can be calculated as

$$\begin{aligned} x_{sep,C,D} &= \sqrt{(\frac{2R_m - a_m}{2})^2 + (d_{\min,m} - d_{\min,s})^2} \\ x_{SC}(d) &= \sqrt{(R_m - a_m + d)^2 + d^2_{\min,m}} \\ x_U(d) &= \sqrt{\left(\frac{a_m}{2} - d\right)^2 + d^2_{\min,s}} \end{aligned} \tag{28}$$

Taking (28) into the above cross-correlated shadow fading model, we can get the standard deviations denoted as $\sigma_{W_{O,D}}$, $\sigma_{W_{N,SC,D}}$ and $\sigma_{W_{N,U,D}}$ of the decomposition components $W_{O,D}$, $W_{N,SC,D}$ and $W_{N,U,D}$, respectively. Thus, the communication outage probability in this area can be expressed as

$$\begin{aligned} &P_{out,C,D}(d) \\ &= 1 - P(SIR_C(x_{SC}(d)) > \Gamma,\ SIR_U(x_U(d)) > \Gamma) \\ &= 1 - \int_{-\infty}^{\infty} \frac{e^{-\frac{t^2}{2\sigma^2 W_{O,D}}}}{\sigma_{W_{O,D}}\sqrt{2\pi}} \Phi\left(\frac{P_{t,m} - PL_m(x_{SC}(d)) - I_{SC} - t - \Gamma}{\sigma_{W_{N,SC,D}}}\right) \\ &\quad \times \Phi\left(\frac{P_{t,s} - PL_s(x_U(d)) - I_U - t - \Gamma}{\sigma_{W_{N,U,D}}}\right) dt \end{aligned} \tag{29}$$

Area E: In the area E, the C-plane of the MR has been handed over to the T-macro-cell. We can get

$$\begin{aligned} x_{sep,C,E} &= \sqrt{(\frac{2R_m - a_m}{2})^2 + (d_{\min,m} - d_{\min,s})^2} \\ x_{TC}(d) &= \sqrt{(R_m - d)^2 + d^2_{\min,m}} \end{aligned} \tag{30}$$

Since in the proposed inter-macro-cell handover scheme the U-plane is always kept connected with the small cell without any handover, the expression of the U-plane signal propagation distance in (28) applies to the area E which is omitted in (30). Similarly, taking (30) into the cross-correlated shadow fading model, the standard deviations denoted as $\sigma_{W_{O,E}}$, $\sigma_{W_{N,TC,E}}$ and $\sigma_{W_{N,U,E}}$ of the decomposition components $W_{O,E}$, $W_{N,TC,E}$ and $W_{N,U,E}$ are obtained, respectively. The communication outage probability in this area is

$$\begin{aligned} &P_{out,C,E}(d) \\ &= 1 - P(SIR_C(x_{TC}(d)) > \Gamma,\ SIR_U(x_U(d)) > \Gamma) \\ &= 1 - \int_{-\infty}^{\infty} \frac{e^{-\frac{t^2}{2\sigma^2 W_{O,E}}}}{\sigma_{W_{O,E}}\sqrt{2\pi}} \Phi\left(\frac{P_{t,m} - PL(x_{TC}(d)) - I_{TC} - t - \Gamma}{\sigma_{W_{N,TC,E}}}\right) \\ &\quad \times \Phi\left(\frac{P_{t,s} - PL(x_U(d)) - I_U - t - \Gamma}{\sigma_{W_{N,U,E}}}\right) dt \end{aligned} \tag{31}$$

No matter whether in the area D or in the area E, the U-plane of the MR is always kept connected with the same small cell without any handover. Hence, the overlapping area U-plane channel capacity can be expressed in a unified form as

$$C_{C,U}(d) = B_{decoupled} \log 2\left(1 + 10^{SIR_U(x_U(d))/10}\right) \tag{32}$$

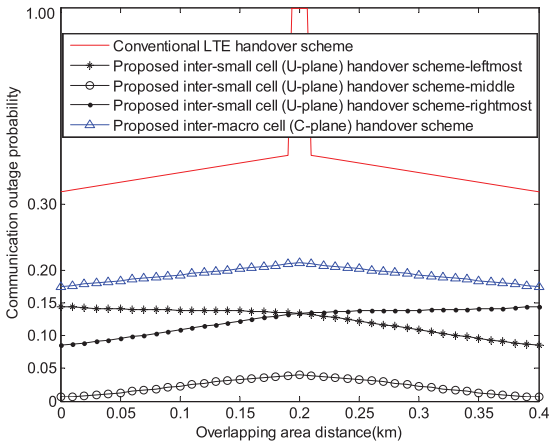

Fig. 8. Communication outage probability comparisons.

In the proposed inter-macro-cell handover scheme, only the C-plane handover happens. Therefore, the handover success probability just depends on the received C-plane signal quality, which can be expressed as

$$P_{success,C}(d) = P_{HO,C}(d) \cdot P\left(SIR_C\left(x_{TC}(d)\right) > \Gamma\right) \quad (33)$$

Based on the derivations in (17) and (20), it is easy to get the expressions of $P_{HO,C}(d)$ and $P\left(SIR_C\left(x_{TC}(d)\right) > \Gamma\right)$, which are not repeated here. Obviously, in terms of the signal quality, the proposed inter-macro-cell handover scheme and the conventional LTE-based handover scheme achieve the same handover success probability.

VI. Numerical Results

In this section, we will present some numerical results to evaluate our proposed schemes. Detailed simulation parameters are listed in TABLE II [31], [32]. To facilitate performance comparisons, the inter-small-cell and inter-macro-cell overlapping area distances are assumed to have the same value. In Fig. 8, the communication outage probabilities in the overlapping areas of different handover schemes are shown. As aforementioned, communication outage probability is related with the C-plane signal quality. For the proposed inter-small-cell handover scheme, the location of the inter-small-cell overlapping area within the associated macro-cell directly determines the C-plane signal quality. Consequently, for clarity, three typical results of the proposed inter-small-cell handover scheme, i.e., the performance of handovers taking place at the middle and two edge inter-small-cell overlapping areas within a macro cell, are illustrated in Fig. 8. Overall the proposed inter-small-cell and inter-macro-cell handover schemes outperform the conventional LTE-based handover scheme. In the conventional LTE-based handover scheme, the U-plane is interrupted in the execution phase corresponding to the center of the overlapping area. While in the proposed schemes, the U-plane is always connected without interruptions. In the CoMP and Bi-casting based inter-small-cell handover scheme, the MR can simultaneously receive two U-plane signals, enhancing the U-plane signal quality. Moreover, since the inter-small-cell overlapping area corresponds to the interior area of the macro cell, the received C-plane signal is also of high quality. Consequently, this scheme achieves the lowest communication outage probability. For the leftmost inter-small-cell overlapping area in the macro cell, as the train moves towards the target small cell, it also gets close to the macro cell. Therefore, as depicted by the curve "'Proposed inter-small cell (U-plane) handover scheme-leftmost" in Fig. 8, the performance ascends as the train runs towards the target small cell. It is opposite for the rightmost inter-small-cell overlapping area that the performance degrades with the train getting close to the target small cell and contrarily being away from the macro cell, which has been described by the curve "Proposed inter-small cell (U-plane) handover scheme-rightmost" in Fig. 8. Based on the parameter setting in Table II, there are six small cells and consequently five inter-small-cell overlapping areas in a macro cell. Precisely, the location of the macro cell base station corresponds to the center of the middle inter-small-cell overlapping area. Therefore, the outage probability in this overlapping area is bilateral symmetry. Besides, the middle one is also the closest to the macro cell. As a consequence, it outperforms the others. In the proposed inter-macro-cell handover scheme, thanks to the small cell elaborately deployed in the inter-macro-cell overlapping area, the consequent enhanced U-plane signal quality greatly reduces the communication outage probability.

Since in the 5G C/U-plane decoupled heterogeneous railway wireless system broader spectra are available, compared with conventional bandwidth limited coupled wireless systems this network can undoubtedly gain higher U-plane channel capacity as shown in Fig. 9(a). To be fair, the U-plane spectrum efficiency comparisons between different handover schemes are also conducted in Fig. 9(b).In the conventional LTE-based handover scheme, the transient U-plane interruption causes a zero U-plane data carrying capability in the overlapping area, while in the proposed inter-macro-cell handover scheme, a small cell is elaborately deployed in the overlapping area to enhance the received U-plane signal quality. The closer to the center of the overlapping area the train is, the higher

TABLE II
Simulation Parameters [31], [32]

Parameters	Values
Frequency of macro-cell	2GHz
Frequency of small-cell	5GHz
Bandwidth of macro-cell $B_{coupled}$	4MHz
Bandwidth of small-cell $B_{decoupled}$	20MHz
Transmit power of macro-cell $P_{t,m}$	43dBm
Transmit power of small-cell $P_{t,s}$	33dBm
Radius of macro-cell R_m	3.2km
Radius of small-cell R_s	800m
Path loss model of macro-cell	Hata
Path loss model of small-cell	M.2135
Shadowing standard deviation of macro-cell	8dB
Shadowing standard deviation of small-cell	6dB
Overlapping area distance a	400m
Handover trigger threshold h	0dB
Outage threshold Γ	8dB
Handover time T_h	0.1s
Mobility v	360km/h
Distance between macro-cell and track $d_{min,m}$	50m
Distance between small-cell and track $d_{min,s}$	30m

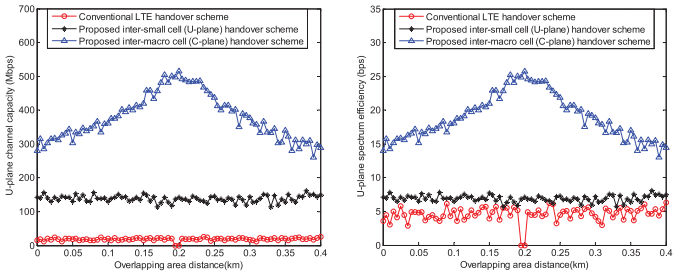

(a) Channel capacity comparison. **(b) Spectrum efficiency comparison.**

Fig. 9. U-plane spectrum efficiency and channel capacity comparisons.

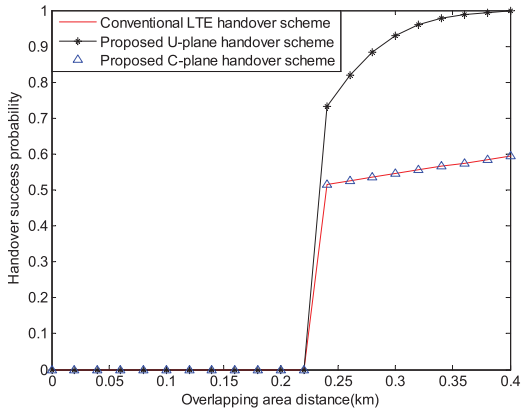

Fig. 10. Handover success probability comparisons.

the received U-plane signal quality gets. Hence, as shown in Fig. 9, the proposed inter-macro-cell handover scheme achieves higher U-plane spectrum efficiency and U-plane channel capacity. In the proposed inter-small-cell handover scheme, owing to the CoMP and Bi-casting technologies that enable the MR to simultaneously receive two U-plane signals, the U-plane spectrum efficiency and U-plane channel capacity are greatly improved by the enhanced U-plane signal quality.

The handover success probability comparisons between different handover schemes are depicted in Fig. 10. Based on the above analysis, we can observe that the proposed inter-macro-cell handover scheme and the conventional LTE-based handover scheme reach the same handover success probability, which is also shown in Fig. 10. Thanks to the enhanced U-plane signal quality in the proposed inter-small-cell handover scheme, the handover success probability is greatly improved.

VII. Conclusions

Due to the limited frequency bandwidth, current narrowband railway wireless communication systems are facing significant challenges in meeting the tremendously growing capacity demands in railway. To leverage both lower and higher frequency bands to increase the system capacity, we proposed a 5G C/U-plane decoupled heterogeneous railway wireless network architecture in our previous study. In this paper, based on this network architecture, we develop a novel mechanism to physically separate and stagger the C-plane and U-plane handovers. In this novel handover scheme, we elaborately deploy a small cell in the overlapping area of macro cells, so that the U-plane can be always kept connected without any handover during the inter-macro-cell (C-plane) handover to achieve the soft and fast handover. Besides, the inter-small-cell overlapping areas correspond to the interior areas of macro cells. Consequently, during the inter-small-cell (U-plane) handover process, the C-plane is kept connected all the time. Without the need to hand over the C-plane, the otherwise intensive C-plane handover signaling is saved, thereby accelerating the handover process. Moreover, in the inter-small-cell handover scheme, the CoMP and Bi-casting technologies are applied to enable the non-interruptible soft handover. Theoretical and numerical results have revealed that the proposed handover schemes can ensure lower communication outage probability and higher U-plane channel capacity than the conventional LTE-based handover scheme. In terms of the handover success probability, the proposed inter-macro-cell handover scheme and the conventional LTE-based handover scheme gain the same performance, while with enhanced U-plane signal quality, the handover success probability in the CoMP and Bi-casting based inter-small-cell handover scheme can be greatly improved.

The C/U-plane decoupled network architecture enjoys great capacity and flexibility advantages by dividing the C-plane and U-plane into different frequency bands and physical nodes. Nevertheless, many efforts are still needed to turn this network architecture into reality. For instance, how to synchronize the separated C-plane signaling with U-plane data is an urgent challenge. Besides, the reduction of backhaul overhead in such networks is also a valuable research direction. In our future study, we will take into account the implement problems of this network architecture.

References

[1] B. Ai *et al.*, "Challenges toward wireless communications for high-speed railway," *IEEE Trans. Intell. Transp. Syst.*, vol. 15, no. 5, pp. 2143–2158, Oct. 2014.

[2] B. Dusza, C. Ide, P.-B. Bök, and C. Wietfeld, "Optimized cross-layer protocol choices for LTE in high-speed vehicular environments," in *Proc. Int. Wireless Commun. Mobile Comput. Conf. (IWCMC)*, Sardinia, Italy, Jul. 2013, pp. 1046–1051.

[3] J. Calle-Sanchez, M. Molina-Garcia, J. I. Alonso, and A. Fernandez-Duran, "Long term evolution in high speed railway environments: Feasibility and challenges," *Bell Labs Tech. J.*, vol. 18, no. 2, pp. 237–253, Sep. 2013.

[4] T. Nakamura *et al.*, "Trends in small cell enhancements in LTE advanced," *IEEE Commun. Mag.*, vol. 51, no. 2, pp. 98–105, Feb. 2013.

[5] C.-X. Wang *et al.*, "Cellular architecture and key technologies for 5G wireless communication networks," *IEEE Commun. Mag.*, vol. 52, no. 2, pp. 122–130, Feb. 2014.

[6] T. S. Rappaport *et al.*, "Millimeter wave mobile communications for 5G cellular: It will work!" *IEEE Access*, vol. 1, pp. 335–349, May 2013.

[7] X. Xu, G. He, S. Zhang, Y. Chen, and S. Xu, "On functionality separation for green mobile networks: Concept study over LTE," *IEEE Commun. Mag.*, vol. 51, no. 5, pp. 82–90, May 2013.

[8] H. Ishii, Y. Kishiyama, and H. Takahashi, "A novel architecture for LTE-B: C-plane/U-plane split and phantom cell concept," in *Proc. IEEE Globecom Workshops*, Anaheim, CA, USA, Dec. 2012, pp. 624–630.

[9] L. Yan and X. Fang, "Decoupled wireless network architecture for high-speed railway," in *Proc. Int. Workshop High Mobility Wireless Commun. (HMWC)*, Shanghai, China, Nov. 2013, pp. 96–100.

[10] L. Yan, X. Fang, and Y. Fang, "Control and data signaling decoupled architecture for railway wireless networks," *IEEE Wireless Commun.*, vol. 22, no. 1, pp. 103–111, Feb. 2015.

[11] L. Yan, X. Fang, G. Min, and Y. Fang, "A low-latency collaborative HARQ scheme for control/user-plane decoupled railway wireless networks," *IEEE Trans. Intell. Transp. Syst.*, vol. 17, no. 8, pp. 2282–2295, Aug. 2016.

[12] L. Yan, X. Fang, Y. Fang, and X. Cheng, "Dual-scheduler design for C/U-plane decoupled railway wireless networks," *IEEE Trans. Mobile Comput.*, to be published. [Online]. Available: http://ieeexplore.ieee.org/document/7563878/
[13] X. Zhu, S. Chen, H. Hu, X. Su, and Y. Shi, "TDD-based mobile communication solutions for high-speed railway scenarios," *IEEE Wireless Commun.*, vol. 20, no. 6, pp. 22–29, Dec. 2013.
[14] (Sep. 2016). *Small Cell*. [Online]. Available: https://en.wikipedia.org/wiki/Small_cell
[15] Q. Wang, G. Ren, and J. Tu, "A soft handover algorithm for TD-LTE system in high-speed railway scenario," in *Proc. IEEE Int. Conf. Signal Process., Commun. Comput. (ICSPCC)*, Xi'an, China, Sep. 2011, pp. 1–4.
[16] W. Luo, R. Zhang, and X. Fang, "A CoMP soft handover scheme for LTE systems in high speed railway," *EURASIP J. Wireless Commun. Netw.*, vol. 1, no. 1, p. 196, Dec. 2012, doi: 10.1186/1687-1499-2012-196.
[17] J. Li, L. Tian, Y. Zhou, and J. Shi, "An adaptive handover trigger scheme for wireless communications on high speed rail," in *Proc. IEEE Int. Conf. Commun. (ICC)*, Ottawa, ON, Canada, Jun. 2012, pp. 5185–5189.
[18] D. Lee *et al.*, "Coordinated multipoint transmission and reception in LTE-advanced: Deployment scenarios and operational challenges," *IEEE Commun. Mag.*, vol. 50, no. 2, pp. 148–155, Feb. 2012.
[19] H. W. Arnold, D. C. Cox, and R. R. Murray, "Macroscopic diversity performance measured in the 800-MHz portable radio communications environment," *IEEE Trans. Antennas Propag.*, vol. 36, no. 2, pp. 277–281, Feb. 1988.
[20] E. Dahlman, S. Parkvall, and J. Sköld, *4G: LTE/LTE-Advanced for Mobile Broadband*. Amsterdam, The Netherlands: Elsevier, 2011.
[21] R. Y. Kim, I. Jung, X. Yang, and C.-C. Chou, "Advanced handover schemes in IMT-advanced systems [WiMAX/LTE update]," *IEEE Commun. Mag.*, vol. 48, no. 8, pp. 78–85, Aug. 2010.
[22] *Feasibility Study for Evolved Universal Terrestrial Radio Access (UTRA) and Universal Terrestrial Radio Access Network (UTRAN) (Release 10)*, document 3GPP TR 25.912 V8.0.0, 2011.
[23] T. S. Rappaport, *Wireless Communications: Principles and Practice*. Upper Saddle River, NJ, USA: Prentice-Hall, 1999.
[24] L. Xiong, Z. Zhong, B. Ai, and H. Wei, "Performance evaluation for high-speed railway mobile communication on HIL simulation platform," in *Proc. 4th IET Int. Conf. Wireless, Mobile Multimedia Netw. (ICWMMN)*, Beijing, China, Nov. 2011, pp. 141–144.
[25] S. S. Szyszkowicz, H. Yanikomeroglu, and J. S. Thompson, "On the feasibility of wireless shadowing correlation models," *IEEE Trans. Veh. Technol.*, vol. 59, no. 9, pp. 4222–4236, Nov. 2010.
[26] J. Weitzen and T. J. Lowe, "Measurement of angular and distance correlation properties of log-normal shadowing at 1900 MHz and its application to design of PCS systems," *IEEE Trans. Veh. Technol.*, vol. 51, no. 2, pp. 265–273, Mar. 2002.
[27] X. Yang, S. Ghaheri-Niri, and R. Tafazolli, "Downlink soft handover gain in CDMA cellular network with cross-correlated shadowing," in *Proc. IEEE VTS 54th Veh. Technol. Conf. (VTC Fall)*, vol. 1. Atlantic City, NJ, USA, 2001, pp. 276–280.
[28] J. Salo, L. Vuokko, H. M. El-Sallabi, and P. Vainikainen, "An additive model as a physical basis for shadow fading," *IEEE Trans. Veh. Technol.*, vol. 56, no. 1, pp. 13–26, Jan. 2007.
[29] K. Yamamoto, A. Kusuda, and S. Yoshida, "Impact of shadowing correlation on coverage of multihop cellular systems," in *Proc. IEEE Int. Conf. Commun. (ICC)*, vol. 10. Istanbul, Turkey, Jun. 2006, pp. 4538–4542.
[30] M. Cheng, X. Fang, and W. Luo, "Beamforming and positioning-assisted handover scheme for long-term evolution system in high-speed railway," *IET Commun.*, vol. 6, no. 15, pp. 2335–2340, Oct. 2012.
[31] G. Hu, A. Huang, R. He, B. Ai, and Z. Chen, "Theory analysis of the handover challenge in express train access networks (ETAN)," *China Commun.*, vol. 11, no. 7, pp. 92–98, Jul. 2014.
[32] L. Tain, Y. Zhou, J. Li, Y. Huang, J. Shi, and J. Zhou, "A novel handover scheme for seamless wireless connectivity in high-speed rail," in *Proc. IEEE 7th Int. Conf. Wireless Mobile Comput., Netw. Commun. (WiMob)*, Seattle, WA, USA, Oct. 2011, pp. 230–236.

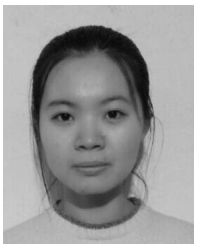

Li Yan (S'14) received the B.E. degree in communication engineering from Southwest Jiaotong University, Chengdu, China, where she is currently working toward the Ph.D. degree with Key Laboratory of Information Coding and Transmission, School of Information Science and Technology. Her research interests include handover, network architecture, and reliable wireless communication for high-speed railway.

Xuming Fang (SM'16) received the B.E. degree in electrical engineering, the M.E. degree in computer engineering, and the Ph.D. degree in communication engineering from Southwest Jiaotong University, Chengdu, China, in 1984, 1989, and 1999, respectively. He was a Faculty Member with the Department of Electrical Engineering, Tongji University, Shanghai, China, in 1984. He then joined the School of Information Science and Technology, Southwest Jiaotong University, where he has been a Professor since 2001 and the Chair of the Department of Communication Engineering since 2006. He held visiting positions with the Institute of Railway Technology, Technical University at Berlin, Berlin, Germany, in 1998 and 1999, and with the Center for Advanced Telecommunication Systems and Services, The University of Texas at Dallas, Richardson, TX, USA, in 2000 and 2001, respectively. He has, to his credit, around 200 high-quality research papers in journals and conference publications. He has authored or co-authored five books or textbooks. His research interests include wireless broadband access control, radio resource management, multihop relay networks, and broadband wireless access for high speed railway. He is the Chair of the IEEE Vehicular Technology Society of Chengdu Chapter.

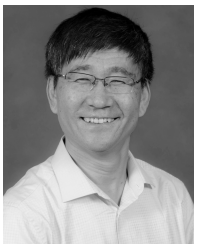

Yuguang Fang (F'08) received the B.S. and M.S. degrees from Qufu Normal University, Shandong, China, in 1987; the Ph.D. degree from Case Western Reserve University in 1994; and the Ph.D. degree from Boston University in 1997. He joined the Department of Electrical and Computer Engineering, University of Florida, in 2000, and has been a Full Professor since 2005. He held a University of Florida Research Foundation (UFRF) Professorship from 2006 to 2009; a Changjiang Scholar Chair Professorship with Xidian University, China, from 2008 to 2011; and a Guest Chair Professorship with Tsinghua University, China, from 2009 to 2012.

Dr. Fang received the U.S. National Science Foundation Career Award in 2001 and the Office of Naval Research Young Investigator Award in 2002, and was a recipient of the Best Paper Award from the IEEE ICNP (2006). He has also received the 2010–2011 UF Doctoral Dissertation Advisor/ Mentoring Award, the 2011 Florida Blue Key/UF Homecoming Distinguished Faculty Award, and the 2009 UF College of Engineering Faculty Mentoring Award. He is an Editor-in-Chief of IEEE TRANSACTIONS ON VEHICULAR TECHNOLOGY, was an Editor-in-Chief of IEEE WIRELESS COMMUNICATIONS (2009–2012), and serves/served on several editorial boards of journals, including IEEE TRANSACTIONS ON MOBILE COMPUTING (2003–2008, 2011–present), IEEE TRANSACTIONS ON COMMUNICATIONS (2000–2011), and IEEE TRANSACTIONS ON WIRELESS COMMUNICATIONS (2002–2009). He has been actively participating in conference organizations, such as serving as the Technical Program Co-Chair at IEEE INOFOCOM2014 and the Technical Program Vice-Chair at IEEE INFOCOM'2005.